Modulated High-Temperature Phases in Brownmillerites $Ca_2(Fe_{1-x}Al_x)_2O_5$

H. Krüger[a,b]

[a] *Research School of Chemistry, The Australian National University, Canberra, Australia*
[b] *Institute of Mineralogy and Petrography, University of Innsbruck, Austria.*

Samples of the title solid solution series (in the range $0 < x < 0.292$) have been investigated using single-crystal X-ray diffraction at room temperature and at high temperatures. Above a phase transition [960(5) K at $x = 0.073(3)$ and 875(5) K at $x = 0.281(4)$] modulated phases are formed. Depending on the composition either commensurate or incommensurate superstructures occur. All of them can be described using the superspace group *Imma(00γ)s00.*

1. Introduction

Brownmillerite (Ca_2AlFeO_5) is one of the four main phases in Portland cement clinkers and therefore its structure, phase transitions and properties are of high interest. The brownmillerite structure type is adopted by many compounds and is among the most frequently studied oxygen-deficient perovskites (for an overview of these materials, see [1] and citations therein). Brownmillerites are a class of oxygen-deficient perovskites, in which the oxygen vacancies are ordered in a way such that chains of tetrahedrally coordinated cations are formed. Their general formula is $A_2B_2O_5$ ($A_2BB'O_5$), where corner-linked [BO_6] octahedra assemble perovskite-like layers, alternating with sheets containing *zweier* single chains of [BO_4] tetrahedra. The octahedral and tetrahedral layers are connected to form a three-dimensional framework, with the *A* ions in interstitial voids. The majority of these compounds adopt the space groups *Pnma* and *I2mb*, as shown in Fig. 1a and 1b, respectively.

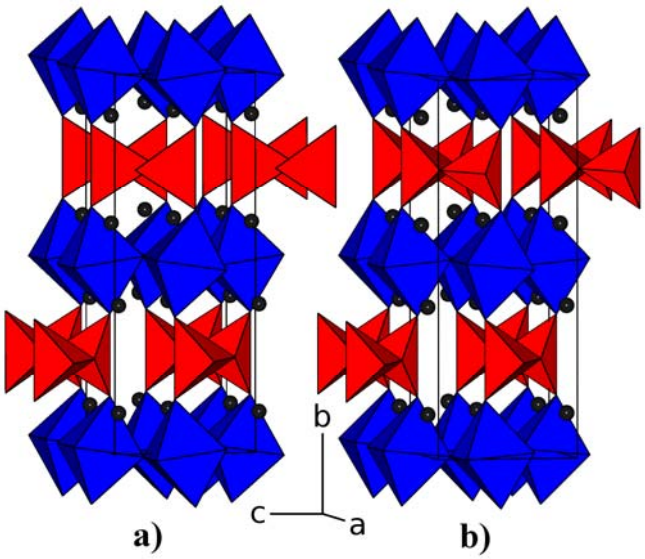

Fig. 1. Brownmillerite structures: space group *Pnma* (a), exhibiting alternating layers of R and L-type chains. Space group *I2mb* (b) showing exclusively one type of tetrahedral chains. The *A* cations are shown as black spheres.

Differences between the two variants can be found in the orientation of the tetrahedral chains: in *Pnma* two possible configurations of the tetrahedral chains (R and L-type) alternate from one to the next layer. Because of the absence of a centre of symmetry only one type of

chain is present in space group *I2mb*. A third frequently reported space group *Imma* requires disorder of R and L-type chains and seems to be an approximation of various superstructures due to ordering of the chains within the layers. Many of such superstructures have been found (see [2] and references therein). As the satellite reflections (arising from an intra-layer order) are rather weak, they are not easy to detect, especially in powder data.

The brownmillerite solid solution series $Ca_2(Fe_{1-x}Al_x)_2O_5$ shows a morphotropic phase transition at ca. $x = 0.28$ from space group *Pnma* to *I2mb* with increasing Al-content. High-temperature (HT) phase transitions in the brownmillerite solid solutions series have been known for a long time and were investigated with differential thermal analysis (DTA) [3], neutron [4] and X-ray powder diffraction [5,6] methods. The space groups reported for the HT phases were *Imma* or *I2mb* [4-6]. Using *in-situ* HT single-crystal X-ray diffraction (XRD) we found the HT structures of $Ca_2Fe_2O_5$ [7] and $Ca_2Al_2O_5$ [8] to be incommensurately modulated. Structural models were derived and refined in superspace group *Imma(00γ)s00* (for details on the superspace approach see [9]). A more detailed single-crystal XRD and HT electron microscopy study on the phase transition of $Ca_2Fe_2O_5$ [10] revealed a temperature range of ca. 25 K, where the *Pnma* and the modulated HT phase coexist. The present study reports new HT single-crystal XRD results on the phase transitions of crystals with the compositions of $x = 0.073(3)$, $x = 0.175(4)$ and $x = 0.281(4)$. Furthermore, samples with $x = 0.121(5)$, $x = 0.171(5)$, $x = 0.229(5)$ and $x = 0.292(4)$ have been examined at room temperature.

2. Sample preparation

Single crystals have been synthesised using a $CaCl_2$ flux [11]. Details on the synthesis can be found in [6].

3. Single-crystal X-ray diffraction

For the HT experiments the crystals have been embedded in 0.1 mm quartz glass mark-tubes (Hilgenberg GmbH, Malsfeld, Germany). The XRD data collections were carried out using a STOE IPDS-2 image plate diffractometer. The chemical composition (Fe:Al ratio) of the samples was determined by structure refinements [12] using room-temperature data. Temperature calibration and computer-controlled series of HT experiments were performed as described in [13]. Each experiment covered a range of at least 20° in ω (with steps of 1.5°). The detector distance was set to 120 mm and the exposure time was 5 min per frame. Data integration for Figs. 2-4 was performed using the same profile parameters and the same scaling factor. The software *integrate* [14] was utilised for the data reduction process. The satellite reflections of the HT modifications were indexed with a modulation wave vector of $\mathbf{q} = \gamma\,\mathbf{c^*}$ [9,14].

4. Results

The Al-content x of all samples was established by crystal-structure refinements using room-temperature XRD data. The results are listed in Table 1. The distribution of Al on the octahedral and tetrahedral sites is not equal. As the results in Tab. 1 show, approximately 3/4 of the Al occupies the tetrahedral site. The preference for the tetrahedral site was reported earlier [6]. The morphotropic phase transition occurs between $0.229 < x < 0.281$. The value published by Redhammer *et al.* is 0.28 for single-crystals, but higher (0.325-0.35) for powders (see [6] for more details and references).

All samples examined at HT show a phase transition to modulated structures, as evident by the occurrence of satellite reflections. As the HT modifications show an *I*-centred lattice, phases adopting space group *Pnma* at room temperature lose their $h+k+l=2n+1$ reflections at

the transition. Consequently, monitoring the intensities of satellites (where present) and *h+k+l=2n+1* reflections gives a powerful tool to observe the coexistence of the phases [10].

4.1 $Ca_2Fe_{0.927}Al_{0.073}O_5$

XRD data of the sample with $x = 0.073(3)$ has been collected in the ranges of 890-970 K (steps of 5 K), 980-1080 K (steps of 20 K), subsequently from 1050-990K (steps of 20 K) and finally from 970-890 K (steps of 5 K). The temperature-dependent intensity changes of selected reflections are shown in Fig. 2. The satellite reflections of the modulated HT phase appear at 960 K. From 990 K their intensities remain constant. The *h+k+l=2n+1* reflections disappear in the transition, as the lattice becomes *I*-centred. Initially strong reflections of this group can be observed up to 1000 K. Consequently, reflections of both phases can be observed over an interval of 40 K. The **q**-vector shows a γ-value of 0.653(1) at 965 K. With higher temperatures the value decreases [0.642(1) at 1080 K]. While cooling γ exhibits a hysteresis, the value stays almost constant down to 965 K [0.644(1)].

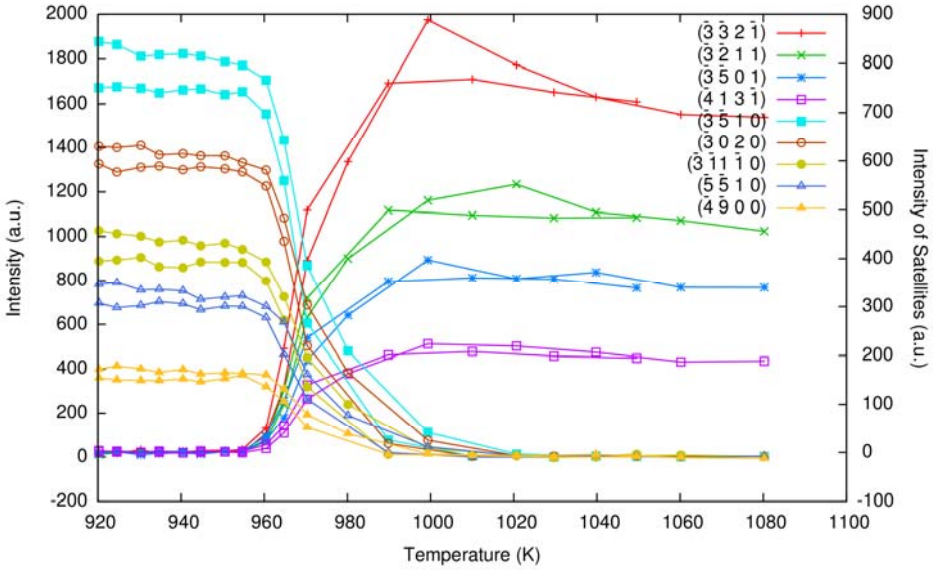

Fig. 2. *Pnma-Imma(00γ)s00* phase transition of $Ca_2Fe_{0.927}Al_{0.073}O_5$. Selected *P*-lattice reflections and satellites show the coexistence of the phases. The heating-cooling cycle does not show a significant hysteresis.

4.2 $Ca_2(Fe_{0.825}Al_{0.175})_2O_5$

A crystal with $x = 0.175(4)$ was investigated at the following temperatures: 875-942 K (5 K steps), 953-923 K (10 K steps), 914-872 K (3 K steps) and 865 K. While heating the transformation sets in between 890 and 894 K (first satellites can be observed at 894 K). The reverse transition (while cooling) shows a small hysteresis, satellites can be observed down to 885 K. At the first appearance of the satellite reflections the **q**-vector shows a commensurate value of $\gamma = 2/3$. Additional experiments show that this value stays unchanged up to 1053 K. Measurements at 1064 and 1073 K show smaller γ-values significantly deviating from 2/3: 0.654(1) and 0.651(1), respectively. This suggests the existence of a commensurate-incommensurate transition between 1053 and 1064 K. The γ-value shows a hysteresis, while cooling the value stays incommensurate down to at least 1013 K.

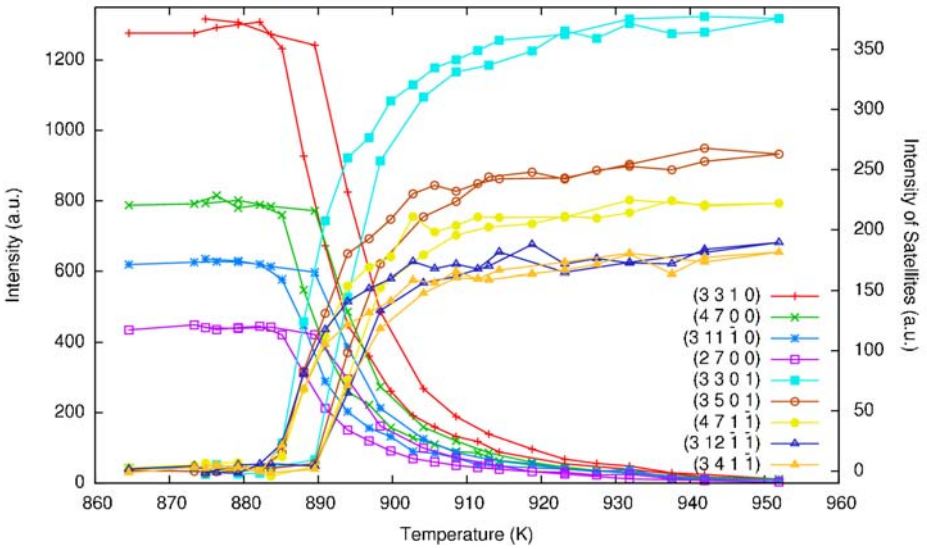

Fig. 3. The *Pnma-Imma(00γ)s00* phase transition of $Ca_2(Fe_{0.825}Al_{0.175})_2O_5$: temperature-dependent changes of selected reflections show a hysteresis of ca. 5 K.

4.3 $Ca_2(Fe_{0.719}Al_{0.281})_2O_5$

The temperature ranges covered by the experiments are: 922-863 K and 876-965 K (steps of 4 K). Crystals with the composition $x = 0.281(4)$ adopt space group *I2mb* at ambient conditions. The transformation to a commensurate superstructure ($\gamma = 2/3$) starts at ca. 870 K. The **q**-vector stays unchanged at least up to 1083 K. Unlike the *I2mb* compounds with $x = 0.175$ and $x = 1$ [8], no significant hysteresis in the phase transition temperature can be detected.

Fig. 4 shows the intensities of selected reflections. In contrast to the compounds $x = 0.147$ and $x = 0.175$, this composition does not show the disappearing of $h+k+l=2n+1$ reflections. Due to the *I*-centred lattice they are already extinct at ambient temperatures. However, some $h+k+l=2n$ reflections show significant changes of their intensities across the phase transition. As this type of modulation (square-wave modulation of occupancies) cannot change its amplitude, the temperature range in which the satellite intensities are increasing can be interpreted as a phase-coexistence range [8].

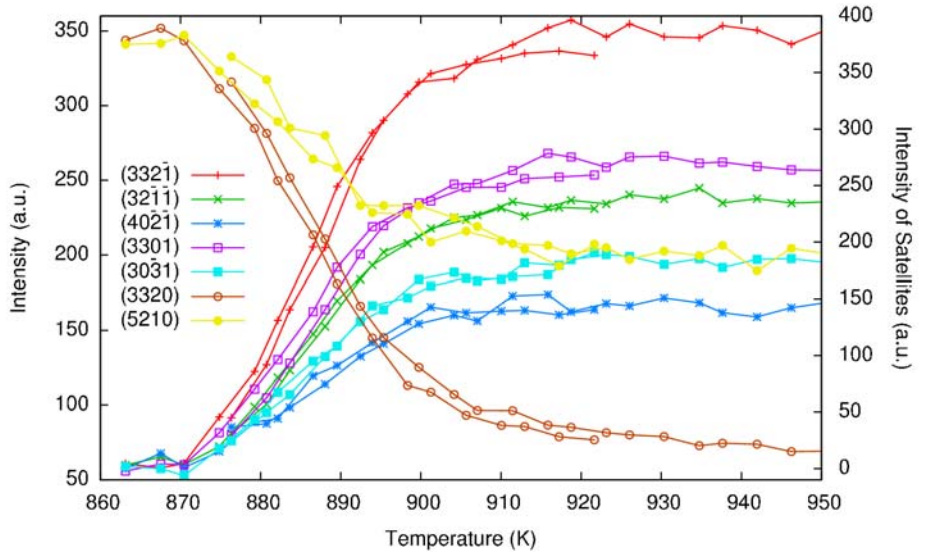

Fig. 4. *I2mb-Imma(00γ)s00* phase transition of $Ca_2(Fe_{0.719}Al_{0.281})_2O_5$: changes of the intensities of selected satellites and main reflections.

5 Discussion

All samples examined at high temperature exhibit a wide (>20 K) range of phase co-existence at the transition as described for $Ca_2Fe_2O_5$ [10]. The phase transition temperatures we found are lower than the ones reported by [6]. This is attributed to the methods used to determine them. The method used in [6] was to monitor a disappearing *P*-reflection [*h+k+l=2n+1*, e.g. (131)]. In this study the first appearance of satellite reflections is used, which will give lower temperatures because of the phase coexistence. However, the values given in Tab. 1 roughly resemble the same slope as given in [6] but shifted to lower temperatures.

The Al end-member (synthesised at 2.5 GPa and 1273 K) shows a large hysteresis in the phase transition temperature [8]. Furthermore, the rate of satellite intensity change shows a difference between the transitions at cooling and heating. Hence the assumed phase coexistence range is 40 K for cooling and 20 K for heating [8]. The **q**-vector of the HT structure shows an incommensurate γ-value close to 0.59. No significant trend of γ could be observed, because the transition temperature is too close to the experimental limit.

Interestingly, the magnitude of the modulation wave vector of both end-members is smaller (Tab. 1) than that of the intermediate samples. Crystals with $x = 0.175$ and $x = 0.281$ show larger and commensurate values. Generally, the value γ seems to decrease with higher temperatures for all samples (except $x = 0.281$, where no decrease could be observed up to the maximum temperature of the experimental setup, which is approx. 1080 K).

A hysteresis in the phase transition temperature was observed for only two samples of the system: $x = 0.0175$ and $x = 1.0$ [8] (see Tab. 1). All other samples do not show any hysteresis in the XRD experiments. However, it has to be noted that the temperature was changed in a step-wise way between the individual XRD experiments, which are performed at a constant temperature (small changes may occur during the image plate readout, due to air draught inside the diffractometer). Obviously, these are not optimal conditions for quantitative and comparable determination of temperature hysteresis in phase transitions. Using DTA at a much faster and well-defined rate of 5 K/min we found a hysteresis of 24 K for the iron end-member [10], which does not show any hysteresis in XRD experiments. Therefore it can be expected that all samples exhibit a hysteresis (using DTA), which is larger than that found in XRD.

Table 1. Aluminium content (*x*), space group (SG), phase transition (PT) temperatures (first appearance of the satellite reflections), hysteresis (by XRD), **q**-vector at PT and amount of Al on the octahedral and tetrahedral site (given in % of a full occupied site).

Al content *x*	SG at RT	PT Temp. [K]	hysteresis [K]	γ	%Al Oct.	%Al Tetr.	Reference
0.000	*Pnma*	960	0	0.607(1)	0.0(0)	0.0(0)	[10]
0.073(3)	*Pnma*	960	0	0.653(1)	4.1(4)	10.6(5)	
0.121(5)	*Pnma*				5.3(7)	18.9(7)	
0.171(5)	*Pnma*				7.2(7)	27.0(8)	
0.175(4)	*Pnma*	890	5	2/3	9.9(6)	25.0(6)	
0.229(5)	*Pnma*				12.6(7)	33.3(7)	
0.281(4)	*I2mb*	875	0	2/3	14.3(6)	41.9(6)	
0.292(4)	*I2mb*				14.6(5)	43.8(6)	
1.000	*I2mb*	1065	100	0.590(2)	100.0(0)	100.0(0)	[8]

6. Conclusions

Basically, the findings of this study agree with the results reported by [6] in the following points: the composition of the morphotropic phase transition, the composition dependence of the HT phase transition temperature of the *Pnma* structure and the fact that Al prefers the tetrahedral site. However, the solid-solution series shows modulated HT structures, which can all be described in superspace group *Imma(00γ)s00*. The HT phases and phase transitions of the investigated samples exhibit interesting features which need further investigation. In particular more single-crystal samples have to be studied *in situ* at high temperatures. Targets of these future studies will be the relationship between composition, temperature and modulation wave vector, as well as the hysteresis observed in some of the samples. To obtain better data on the temperature hysteresis dedicated DTA experiments are planned.

Acknowledgments

HK acknowledges financial support of the Austrian Science Fund (FWF): J2996-N19. HK also thanks G. Redhammer for providing the sample material, and R. Whitfield for proofreading the manuscript.

References

[1] Antipov E V, Abakumov A M and Istomin S Y 2008 *Inorg. Chem.* **47** 8543
[2] D'Hondt H, Abakumov A M, Hadermann J, Kalyuzhnaya A S, Rozova M G, Antipov E V and Tendeloo G V 2008 *Chem. Mater.* **20** 7188
[3] Woermann E, Eysel W and Hahn T 1968 *Proceedings of the 5th International Symposium on the Chemistry of Cement* p 54.
[4] Berastegui P, Eriksson S-G and Hull S 1999 *Mater. Res. Bull.* **34** 303
[5] Fukuda K and Ando H 2002 *J. Am. Ceram. Soc.* **85** 1300
[6] Redhammer G J, Tippelt G, Roth G and Amthauer G 2004 *Am. Mineral.* **89** 405
[7] Krüger H and Kahlenberg V 2005 *Acta Crystallogr. B* **61** 656
[8] Lazić B, Krüger H, Kahlenberg V, Konzett J and Kaindl R 2008 *Acta Crystallogr. B* **64** 417
[9] Janssen T, Janner A, Looijenga-Vos A and de Wolff P M 2004 Incommensurate and commensurate modulated structures (Chapter 9.8 of *International Tables for Crystallography,* vol C) ed. E Prince (Dordrecht: Kluwer Academic Publishers) pp 907-955.
[10] Krüger H, Kahlenberg V, Petříček V, Philipp F and Wertl W 2009 *J. Solid State Chem.* **182** 1515
[11] Kahlenberg V and Fischer R X 2000 *Eur. J. Mineral.* **12** 129
[12] Petříček V, Dušek M and Palatinus L 2006 *Jana2006. The crystallographic computing system* (Prague: Institute of Physics).
[13] Krüger H and Breil L 2009 *J. Appl. Crystallogr.* **42** 140
[14] Stoe and Cie GmbH 2006 *Integrate 1.39* (Darmstadt).